

# Small lymphocytic lymphoma, marginal zone B-cell lymphoma, and mantle cell lymphoma exhibit distinct gene-expression profiles allowing molecular diagnosis

Catherine Thieblemont, Valéry Nasser, Pascale Felman, Karen Leroy, Sophie Gazzo, Evelyne Callet-Bauchu, Béatrice Lloriod, Samuel Granjeaud, Philippe Gaulard, Corinne Haioun, Alexandra Traverse-Glehen, Lucile Baseggio, François Bertucci, Daniel Birnbaum, Florence Magrangeas, Stéphane Minvielle, Hervé Avet-Loiseau, Gilles Salles, Bertrand Coiffier, Françoise Berger, and Rémi Houlgatte

**Non-germinal center small B-cell lymphomas represent a heterogeneous group of non-Hodgkin lymphomas, the most frequent histologic subtypes being small lymphocytic lymphoma (SLL), splenic marginal zone B-cell lymphoma (MZL), and mantle cell lymphoma (MCL). In order to identify genomic signatures specific for each disease, we analyzed 128 primary tumors using high-density microarrays. Several clusters of genes significantly discriminated the 3 histologic subtypes. Genes associated with cell ad-**

**hesion, angiogenesis, and inhibition of apoptosis were up-regulated in SLL. Genes associated with intracellular signaling via the AKT1 pathway were up-regulated in splenic MZL. Genes associated with cell cycle control and multidrug resistance were up-regulated in MCL. Using 44 genes selected within the gene clusters discriminant for the 3 lymphoma subtypes, we generated a class prediction score that allowed us to classify the 3 entities in 96% of the cases, including borderline cases. Whereas specific tran-**

**scriptional profiles easily distinguished all MZL samples, SLL samples, and most of the MCL samples into separate groups, few MCL cases exhibited MZL-type transcriptional profiles. This study demonstrates that SLL, splenic MZL, and MCL possess specific transcriptional profiles that may be relevant to the pathogenesis and the diagnosis of these histologic subtypes. (Blood. 2004;103:2727-2737)**

© 2004 by The American Society of Hematology

## Introduction

Gene-expression profiling has been used extensively for diffuse large B-cell lymphoma analysis during the past 3 years,<sup>1-3</sup> contributing to a dramatic increase of knowledge for B-cell lymphoid tumorigenesis.<sup>4</sup> Lymphoma oncogenesis involves disruption of normal B-cell differentiation at different stages. The non-germinal center small B-cell lymphomas<sup>5</sup> represent a heterogeneous group of B-cell lymphoid neoplasms related to different cells of origin, the most frequent subtypes being small lymphocytic lymphoma (SLL) which is molecularly and clinically related to chronic lymphocytic leukemia (CLL), marginal zone B-cell lymphoma (MZL), and mantle cell lymphoma (MCL), which is associated with t(11;14)(q13;q32) resulting in cyclin D1 overexpression.

These 3 lymphoma entities have a very different clinical outcome but may be difficult to distinguish either histologically or clinically. Moreover, in spite of multifaceted phenotypic characterization, there are some "borderline" cases without definitive classification. The recent studies using gene-expression profiling have established that lymphomas and leukemias that are difficult to distinguish morphologically can nevertheless be distinguished molecularly.<sup>1-3,6-8</sup>

The goal of our study was to characterize the molecular pathways specifically involved in SLL, splenic MZL, and MCL

using gene-expression profiling. The results showed that different biologic pathways were altered in these malignancies, each disease being characterized by a specific genomic signature. According to the expression of 44 genes selected within the gene clusters discriminant for the 3 lymphoma subtypes, we generated a class prediction score in order to classify all the cases involved in the study, including the few borderline cases. Moreover, MZL and SLL samples, and most of the MCL samples, could be distinguished according to their transcriptional profiles as distinct entities. However, a few MCL cases exhibited MZL-type transcriptional profiles.

## Patients, materials, and methods

### Selection of patients

Fresh-frozen tumor biopsies and clinical data were obtained retrospectively from 121 untreated patients of 3 different institutions after complete morphologic analysis, including cytologic, immunologic, cytogenetic (conventional cytogenetic and fluorescent in situ hybridization [FISH]), and/or molecular analysis, to assess the diagnosis of typical SLL, typical MZL, or MCL. All patients had signed informed consent for biopsy analysis.

From the Service d'Hématologie, the Service d'Hématologie cellulaire, and the Service d'anatomie pathologique, Centre Hospitalier Lyon-Sud, Hospices civils de Lyon, Pierre-Bénite; Equipe d'Accueil "Pathologie des cellules lymphoïdes," Université Claude Bernard-Lyon 1, Lyon; TAGC, INSERM ERM206, and the Département d'oncologie moléculaire, Institut Paoli-Calmettes, Marseille; Département de Pathologie, EA2348, Hôpital Henri Mondor, AP-HP, and the Service d'Hématologie, Hôpital Henri Mondor, Créteil; and INSERM U463, Nantes, France.

Submitted June 30, 2003; accepted September 29, 2003. Prepublished online as *Blood* First Edition Paper, November 20, 2003; DOI 10.1182/blood-2003-06-2160.

Supported by the Ligue Contre le Cancer: Départements du Rhône, de la

Saône et Loire, de la Drôme et de l'Ardèche. V.N. was supported by the Association pour la Recherche sur le Cancer and the Paoli-Calmettes Institut.

The online version of this article contains a data supplement.

**Reprints:** Catherine Thieblemont, Service d'hématologie, Pavillon 1F, Centre Hospitalier Lyon-Sud 69495 Pierre-Bénite Cedex, France; e-mail: catherine.thieblemont@chu-lyon.fr.

The publication costs of this article were defrayed in part by page charge payment. Therefore, and solely to indicate this fact, this article is hereby marked "advertisement" in accordance with 18 U.S.C. section 1734.

© 2004 by The American Society of Hematology

Morphologic characteristics of the patients are shown in Table 1. Only 2 patients with SLL had more than  $10 \times 10^9/L$  circulating peripheral blood lymphoma cells<sup>9</sup> ( $13 \times 10^9/L$  and  $14 \times 10^9/L$ , respectively). All patients with MZL had a splenic MZL except 2 who had nodal MZL.<sup>10</sup> Two patients with splenic MZL with the expected immunophenotype and morphology presented a t(11;14) translocation with cyclin D1 overexpression and unmutated IgV<sub>H</sub> gene status. All MCL samples were controlled for cyclin D1 overexpression by competitive reverse transcriptase–polymerase chain reaction (RT-PCR).<sup>11</sup> Three of the patients with MCL lacked CD5 expression but were typical MCL when considering histology, cytology, and cytogenetic analysis. This group of patients corresponded to the preliminary group or learning set.

Before sample processing, morphologic review of all the cases was performed (F.B., P.F., P.G., E.C.-B.) and 6 cases were classified as borderline (Table 2). Among them, 4 MZL cases were secondarily classified as borderline SLL-MZL because of a very diffuse pattern of splenic infiltration and CD5<sup>+</sup> expression for 3 of those cases, and 2 MCL cases were secondarily classified as borderline MCL-MZL because of lack of MCL morphologic characteristics. These 6 borderline cases were then analyzed separately. The presence of somatic mutations of IgV<sub>H</sub> genes was determined in all available samples.<sup>12</sup>

### Isolation of total RNA

Tumor material was snap frozen in liquid nitrogen. Frozen sections were stained with hematoxylin and eosin and only samples that had more than 50% tumor cells were selected. Ten 50- $\mu$ m sections were used for the isolation of RNA. Total RNA was isolated using a guanidium isothiocyanate–based method (Trizol reagent; Gibco BRL, Grand Island, NY). Total RNA obtained from 2 cell lines of mantle cell type (GRANTA and

NCEB) was also extracted. Total RNA was treated with DNase to minimize genomic DNA contamination (DNA free; Ambion, Cambridgeshire, United Kingdom), the RNA was then dissolved in RNase-free water to a final concentration of 0.5  $\mu$ g/ $\mu$ L. Quality and quantity controls were assessed by optical density (OD) 260/280 ratios and by electrophoresis (Agilent 2100 Bioanalyzer; Agilent, Massy, France). Twenty-two samples from the learning set were not accepted for further experimentation, 3 because of insufficient quantity and 19 because of insufficient quality. A total of 101 samples were available for microarray hybridization (99 patient samples [93 typical and 6 borderline cases] and 2 cell lines).

### cDNA microarrays

The microarrays included 6692 clones of complementary DNA, 2500 of which were related with carcinogenesis, and 427 controls.<sup>13</sup> The cDNA clones were obtained through a selection of IMAGE clones using expressed sequence tag (EST) databases, and were amplified as previously described. PCR products were spotted onto nylon membranes using a 64 plain pins Microgrid II printer (Apogent Discoveries, Hudson, NY). The amounts of target cDNA accessible to probe hybridization were controlled in each spot using the hybridization of an oligonucleotide common to each cDNA<sup>13</sup> performed previously to the sample hybridization.

### Labeling and hybridization to the microarray

cDNA synthesis, radioactive-labeling, hybridization, and washing of the cDNA microarray membranes were performed according to procedures available on the web at <http://tagc.univ-mrs.fr/pub>. Briefly, 2.0  $\mu$ g total RNA was used as a template for cDNA synthesis in the presence of <sup>33</sup>P]

**Table 1. Phenotypic characteristics of the 122 patients whose biopsy has been hybridized on microarrays**

Patients	Total N = 122	B-CLL/SLL n = 31		Splenic MZL* n = 37		MCL n = 56	
		Preliminary group, n = 19 (%)	Validation group, n = 10 (%)	Preliminary group, n = 29 (%)	Validation group, n = 8 (%)	Preliminary group, n = 45 (%)	Validation group, n = 11 (%)
<b>Samples</b>							
Lymph node	77 (63)	19 (100)	9 (90)	2 (6)†	0	38 (85)	9 (82)
Spleen	33 (27)	0	1 (10)	19 (66)	8 (100)	5 (11)	0
Blood	9 (7)	0	0	8 (28)	0	1 (2)	0
Others: tonsil	3 (3)	0	0	0	0	1 (2)	2 (18)
<b>Immunophenotype</b>	122 (100)						
CD19/CD20 <sup>+</sup>		19 (100)	9 (100)	29 (100)	8 (100)	38 (100)	9 (100)
CD5 <sup>+</sup>		19 (100)	9 (100)	5 (17)	0	35 (92)	9 (100)
CD23 <sup>+</sup>		19 (100)	9 (100)	0	0	0	0
CD43 <sup>+</sup>		19 (100)	9 (100)	0	0	38 (100)	9 (100)
CD10 <sup>+</sup>		0	0	0	0	—	—
<b>Cytogenetic features</b>	96 (79)	19	2	29	2	34	2
del 13q		1 (5)	0	1 (3)	0	0	0
+12		9 (47)	0	0	0	0	0
del 11q		4 (21)	0	0	0	1 (3)	0
+3 or +3q		0	0	8 (27)	0	2 (6)	0
del 7q		0	0	5 (17)	0	0	0
t(11;14)		0	—	2 (11)	0/2	34/34 (100)	2/2 (100)
<b>Molecular features</b>							
Cyclin D1 +++	58 (46)	—	—	2 (11)	0	45 (100)	9 (100)
<b>Ig mutation status</b>							
Mutated (< 98)	36 (29)	5 (26)	1 (10)	19 (66)	4 (50)	7 (15)	0
Unmutated ( $\geq$ 98%)	63 (52)	12 (63)	8 (80)	8* (27)	4 (50)	22 (49)	9 (82)
Not done	23 (19)	2 (11)	1 (10)	2 (7)	0	16 (36)	2 (8)
<b>Circulating peripheral</b>							
blood lymphoma							
cells > $10 \times 10^9/L$		2/19 (10)	0/8	13 (45)	0/6	1/45	0/7

Blood samples were used for microarray hybridization when frozen material (spleen biopsy [n = 8] for splenic MZL or node biopsy [n = 1] for MCL) was not available for RNA extraction. All blood samples contained more than 50% lymphoma cells. — indicates not done.

\*bcl-6 immunostaining was negative.

†Two patients presented a nodal MZL and not splenic MZL at diagnosis.

**Table 2. Clinical and morphologic characteristics of the borderline cases**

	Case 1 SLL/MZL	Case 2 SLL/MZL	Case 3 SLL/MZL	Case 4 SLL/MZL	Case 5 MZL/MCL	Case 6 MZL/MCL
<b>Clinical features</b>						
Sites of involvement	Spleen Bone marrow	Spleen Bone marrow Blood	Spleen Bone marrow Blood	Spleen Bone marrow	Nodes spleen Bone marrow	Nodes spleen Bone marrow
Lymphocytosis	3 × 10 <sup>9</sup> /L	12 × 10 <sup>9</sup> /L	8 × 10 <sup>9</sup> /L	80 × 10 <sup>9</sup> /L	4 × 10 <sup>9</sup> /L	3 × 10 <sup>9</sup> /L
LDH	Elevated	Elevated	Normal	Elevated	Normal	Elevated
B2 microglobulin, g/L	3.1	6	1.9	3.2	4.3	3.1
Monoclonal component	M Kappa-29.3 g/L	G Lamda-4 g/L	0	0	0	0
Follow-up, years	2.26	148 days	3.55	1.94	121 days	2.83
Status at last follow-up	Alive	Dead (Neuro)	Alive	Dead	Dead	Alive
Histology	Diffuse infiltration of red pulp by small lympho-plasmacytic cells	Diffuse infiltration of small plasmacytoid cells	Micronodular infiltration of small cells	Diffuse infiltration of red pulp by small round cells; nodular pattern in splenic hilar LN	Micronodular and diffuse infiltration of round cells and centrocytic cells	Diffuse infiltration of small round cells, numerous mitoses
Lymphocyte cytology	Lympho-plasmacytic cells, MZL type	Atypical CLL cells (clumped chromatin, plasmacytoid differentiation, smudge cells)	Clumped chromatin, no smudge cells	Clumped chromatin, some smudge cells	Heterogeneous in size (small to large), basophilic cytoplasm	Small cells with regular nucleus
Immunophenotype of B cells	CD5 <sup>+</sup> CD23 <sup>-</sup>	CD5 <sup>+</sup> CD23 <sup>-</sup> CD43 <sup>+</sup> wk	CD5 <sup>+</sup> CD23 <sup>+</sup> wk CD43 <sup>+</sup> wk Slg <sup>+++</sup> FMC7 <sup>+</sup> , CD22 <sup>++</sup>	CD5 <sup>+</sup> CD23 <sup>-</sup> CD43 <sup>-</sup> Slg <sup>+++</sup> , MC7 <sup>+</sup> , CD22 <sup>++</sup>	CD5 <sup>+</sup> CD23 <sup>-</sup> CD43 <sup>-</sup>	CD5 <sup>+</sup> CD23 <sup>-</sup> CD43 <sup>+</sup>
Cytogenetics	+12 del13q	Complex without recurrent abnormalities	+12 +18	Complex with +3q	Complex with t(11;14)	No t(11;14) but very rare mitoses
IgV <sub>H</sub> mutational status	Mutated	Mutated	Mutated	Mutated	Mutated	Not mutated
Cyclin D1	Not applicable	Not applicable	Not applicable	Not applicable	++	++
Site of biopsy	Spleen	Spleen	Spleen	Spleen	Spleen	Node

+, ++, and +++ correspond to the expression level of the immunostaining.  
LN indicates lymph node; LDH, lactodehydrogenase.

dATP (Amersham Pharmacia Biotech, Bucks, United Kingdom) to produce labeled cDNA. The labeled targets were purified using spin columns (Sephadex G50; Roche Diagnostics, Meylan, France). Hybridizations were carried out during 48 hours at 68°C in a rotation hybridization oven using 30 × 10<sup>6</sup> cpm of the probe in a final volume of 300 μL buffer. The membranes were then washed at 68°C twice during 3 hours, exposed for 24 and 48 hours on a radioimager, and scanned (Fuji Bas 5000; Raytest, Paris, France). Signal intensities on scanned images were quantified (ArrayGauge software v1.3; Fuji, Paris, France). The values were corrected for background level, normalized for the amount of spotted cDNA and the variability of experimental conditions, and log-transformed.<sup>14</sup> From the initial 6692 clones, 2533 were significantly expressed in a majority of the samples.

### Validation strategy

To investigate the diagnostic value of the gene-expression profile, an additional 29 untreated patients were independently selected for a validation group on the same criteria as those described for the preliminary group. Morphologic characteristics are detailed in Table 1. Samples were processed independently from the preliminary group using the same experimental protocol and the assignment to lymphoma subtypes was allocated in a blinded fashion.

### Statistical analysis

Before analysis, the reproducibility of the experiments was verified by comparing 2 hybridizations of samples prepared from the same RNA on 2

different arrays. Twenty-one samples were then hybridized twice. The reproducibility of the experiments between the preliminary group and the validation group was also verified with 2 samples hybridized in both groups. Regarding the analysis, these 2 samples were included in the preliminary group and not in the validation group. In every case, the results showed good reproducibility with correlation coefficients of 0.98 (data not shown).

Average linkage, unsupervised, hierarchical clustering was applied to preliminary group samples to investigate relationships between samples and relationships between genes. We used the Cluster program and displayed results with the Treeview program (M. Eisen, University of California, Berkeley; <http://www.microarrays.org/software>).<sup>15</sup>

Genes discriminating particular lymphomas subtypes (SLL, splenic MZL, MCL) were searched in the preliminary samples using a signal-to-noise calculation with a discriminating score (DS) equal to  $(\mu_1 - \mu_2) / (\sigma_1 + \sigma_2)$ ,<sup>16,17</sup> where  $\mu_1$  and  $\sigma_1$  represent, respectively, mean and standard deviation of the expression levels of the genes in the group of the lymphoma subtype 1, and  $\mu_2$  and  $\sigma_2$  represent, respectively, mean and standard deviation of the expression levels of the genes in the other samples. One hundred random permutations of the samples were used to calculate the significant level of risk at 1 of 10 000, resulting in less than one false-positive gene. A given gene was considered to characterize a particular subtype when it was overexpressed in this subtype in comparison to the 2 other subtypes. A very similar set of genes could also be detected by a *t* statistic with Bonferroni correction.<sup>18</sup>

A multiple class predictor was built using the method described by Sorlie et al:<sup>19</sup> (1) clusters of genes discriminating tumor subtypes were

selected, (2) a mean profile was determined for each tumor subtype, and (3) correlations between individual samples and tumor subtypes were calculated. A high correlation between one sample and one tumor-subtype mean profile reflects the similarity between that sample and the tumor subtype. Selected clusters were those containing more than 80% of genes distinguishing a particular lymphoma subtype and associated with a correlation superior to 0.66. This correlation threshold allowed the separation between splenic and MZL signatures, which were strongly associated with the tissue of origin of the MZL samples (mainly spleen). Subtype-specific mean profiles were determined using the mean expression values observed in all samples of this subtype for each selected gene. Pearson correlations between the expression of the selected genes in each sample and the 3 mean profiles were calculated ( $R_{SLL}$ ,  $R_{MCL}$ ,  $R_{MZL}$ ). Correlations of more than 0.4 were considered as significant with a 5% risk. This threshold was calculated by generating bootstrapped profiles, where expression of each gene was randomly chosen from all the observed values for that gene in samples of any subtype. Samples exhibiting no significant correlation with any subtype profile were considered as unpredictable. None of the samples exhibited a significant correlation with 2 subtype profiles.

### Protein validation (immunohistochemistry)

The potential extension of microarray-based diagnosis prediction was further explored using immunohistochemistry. We chose one molecule for each lymphoma subtype because of the very high discriminating score for each specific disease and because of the commercial availability of antibodies: L-selectin for SLL (1/20; Dako SA, Trappes, France), pAKT1 protein for splenic MZL (1/100; Upstate Cell Signaling, Euromedex, Strasbourg, France), and glutathione S-transferase (GSTpi) (1/200; Tebu International, Le Perray en Yveline, France) for MCL. We used formalin-fixed, paraffin-embedded sections for glutathione S-transferase pi and pAKT1 analysis, and frozen sections for L-selectin analysis. The formalin-fixed, paraffin-embedded sections were subjected to antigen retrieval by boiling in a microwave for 30 minutes in 0.01 M sodium citrate buffer (pH 6.0) and then exposed to 3% hydrogen peroxide diluted in water for 20 minutes at room temperature. Immunohistochemistry analysis was realized using a Ventana system according to the manufacturer's instructions, except for pAKT1 incubated at 4°C overnight and for which a streptavidin-biotin system (Dako Duet kit) was used. Fifteen samples (5 for each entity) were analyzed.

## Results

### Categorization of gene-expression signatures

Total RNA of each normal and malignant sample was isolated and used to generate a radio-labeled cDNA, which was hybridized to microarrays containing 6692 human cDNA clones. Radioactive dot intensities of scanned images were quantified. The overall expression patterns were first analyzed using hierarchical clustering in an unsupervised fashion to group the 122 analyses of the 101 preliminary group samples according to the gene-expression profiles of the 2533 expressed genes. Figure 1 presents the variation in gene-expression patterns in the samples. Examination of the data on the vertical axis highlighted clusters of correlated genes defining gene-expression signatures corresponding either to the cell type or the tissue type in which its component was expressed (eg, the "T-cell" signature, the "SPLEEN" signature) or to the biologic process in which its component genes are known to function (eg, the "EARLY RESPONSE" signature; Figure 2). The "SPLEEN" cluster-grouped genes expressed only in spleen samples, whatever the disease subtype, and included genes related to red cells (*hemoglobin zeta*  $\zeta$ , *EPB4.1-like2*, *KLF1*, for example). A "STROMAL" cluster associating genes such as *COL1A1*, *COL1A2*, *COL3A1*, *MMP2*, *MMP9*, *TIMP3*, and *VCAM1* was expressed in

nodal and splenic samples as compared with the cell lines and the blood samples. Cyclin D1 gene expression correlated with that of other genes including *MACS*, *ETV4*, *JUP* (junction plakoglobin), *EHD1* to constitute an independent and small gene cluster. Three lymphoma subtype-specific clusters could be detected: the SLL cluster (interleukin 4 [IL4] receptor, L-selectin, RAS-GAP1, titin), the MZL cluster (*AKT1*, *AGER*, *S100A9*, *ZFP36*), and the MCL cluster (*GST pi*, *DNMT1*, *PCNA*, *CDK4*).

Although no information on the identity of the samples was used in the clustering, the algorithm could segregate, with few exceptions, the SLL, splenic MZL, and MCL subtypes. Clearly, it appeared that several of the previously identified gene clusters were differentially expressed between the SLL, the splenic MZL, and the MCL categories. SLL samples overexpressed the SLL gene cluster. Splenic MZL samples overexpressed genes grouped in a cluster including *AKT1*, *S100A* proteins, and *AGER*, and genes grouped in the cluster related to the splenic tissue. The MCL cluster genes were overexpressed in the MCL samples, as well as in the MCL cell lines. MCL samples also overexpressed genes related to the stroma.

### Gene-expression-based diagnostic predictor

We used the preliminary collection of samples belonging to known classes to create a "diagnostic predictor" based on the gene-expression profiles. Using a discriminating score<sup>16</sup> and a permutation test to assess each gene's individual ability to distinguish the lymphoma subtype,<sup>20</sup> we found that 415 genes were significantly ( $P < .0001$ , 0.75 false-positive gene) correlated with the SLL, splenic MZL, or MCL subtype (Table 3). We ranked the informative genes into 3 groups, the higher score indicating the greater ability to differentiate one sample between the 3 profiles. The list of genes is available on the web at <http://tagc.univ-mrs.fr/pub>.

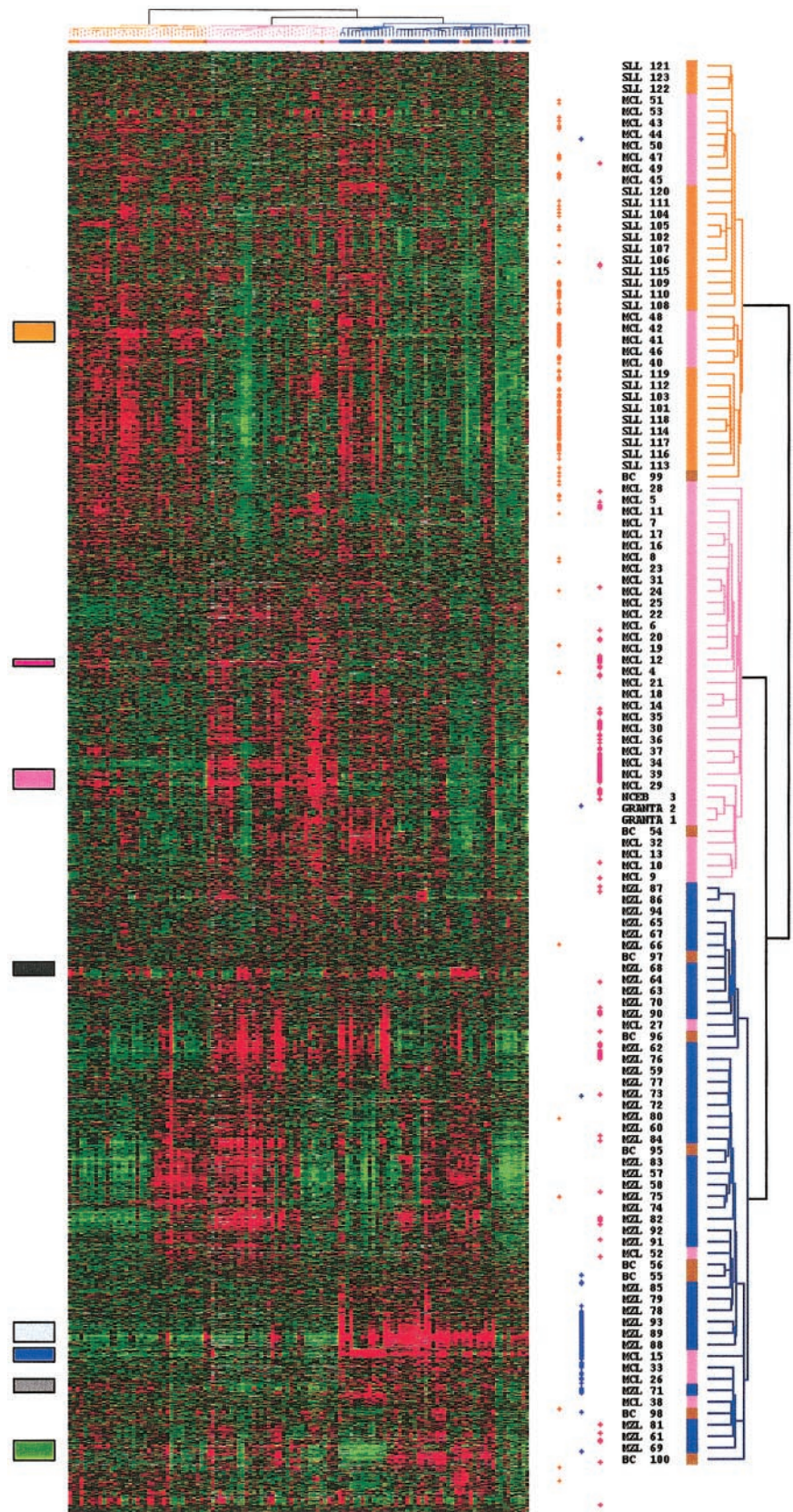
SLL discriminating genes grouped 178 genes related to cell adhesion (*P-* and *L-selectin*, *integrin  $\alpha 5$* , *LAMR1*, *COL4A4*, *COL18A1*, *CCR2*, *MIF*), to angiogenesis (angiopoietin-like 3, *FIGF*), and to cell fate (*notch 4*, *IL4R*, *TNFR17*). Several of these genes (*BCL2*, *survivin*, and *TNFR10*) were related to inhibition of apoptosis, a major feature in CLL/SLL. Several genes related to the cell cycle such as *cyclin H* and *cyclin D2* and *D3*, *RB1*, *ELF1*, and *TGFB1&2* were also overexpressed.

MCL discriminating genes regrouped 154 genes. Most of these genes could be related to 3 functions: cell proliferation, gene transcription, and drug resistance. Cell proliferation genes represented the most important group of genes including *PCNA*, *CDK4*, *cyclins F*, *DNMT1*, *CDC46*, *MYBL2*, and *topoisomerase A2*. Genes related to transcription activity were *TFAP2A*, *TCF3*, *SRF*, *NFE2L3*, *SMARCA4*. Several genes related to drug resistance were overexpressed in MCL: *GST pi* and 2 *MDR/ATP-binding cassette (ABC)* membrane proteins (*ABCG2* and *ABCC5*). All MCL samples overexpressed cyclin D1 cluster independently from the other specific MCL genes.

Splenic MZL discriminating genes regrouped 83 genes from 2 clusters. One of the 2 clusters was specifically associated with the MZL signature, whatever the site of the biopsy (spleen, node, or blood). These genes were involved in intracellular signaling (*AKT1*, *AGER*) or transcription (*TFCP2*, *MXI1*). Several *S100A* proteins (*S100 A8* and *A9* [calgranulin a and b]) positively discriminated the MZL samples. The second splenic MZL signature corresponded to the "SPLEEN" cluster and was related to genes expressed by cells others than lymphoma B-cells such as red cells (eg, hemoglobin zeta) and T cells, considered as contaminant cells interfering with the MZL signature. Genes belonging to this cluster were excluded in the final diagnostic predictor. This led to a



**Figure 1. Hierarchical clustering of gene-expression data.** Measurements of gene expression from 122 microarray analyses of the 101 nonfollicular small B-cell lymphoma samples of the preliminary group, and the 2 mantle cell lines (NCEB; GRANTA) are depicted. Each column represents the genomic profile of the 2533 expressed genes for one tumor, and each row represents the relative level of expression of one cDNA clone. Red indicates a high level of expression of messenger RNA of the given gene in the tumor, as compared with the median value of this gene, and green indicates a low level of expression, according to the color scale. Gray indicates missing data. Correlated genes are grouped across the samples into clusters localized by the colored boxes. The dendrogram, reported also at the top of the hierarchical clustering, lists the samples studied and provides a measure of the relatedness of gene expression in each sample. SLL cases are colored in orange, MZL cases in blue, MCL cases in pink, and cases reclassified as borderline cases in brown. The dots at the right side of the hierarchical clustering represent the genes that significantly discriminate the 3 entities. The orange dots represent the genes that discriminated the SLL entity, the blue dots the MZL entity, and the pink dots the MCL entity.



total of 47 MZL discriminating genes, and these genes shared weaker discriminating scores than SLL or MCL discriminating genes. For example, the top 100 discriminating scores contained only 6 genes discriminating MZL samples.

In order to create a multiclass predictor, we used a method derived from Sorlie et al.<sup>19</sup> This method first selects genes from subtype-specific clusters to generate the predictor. Second, the inclusion of a gene in a given class is determined by the



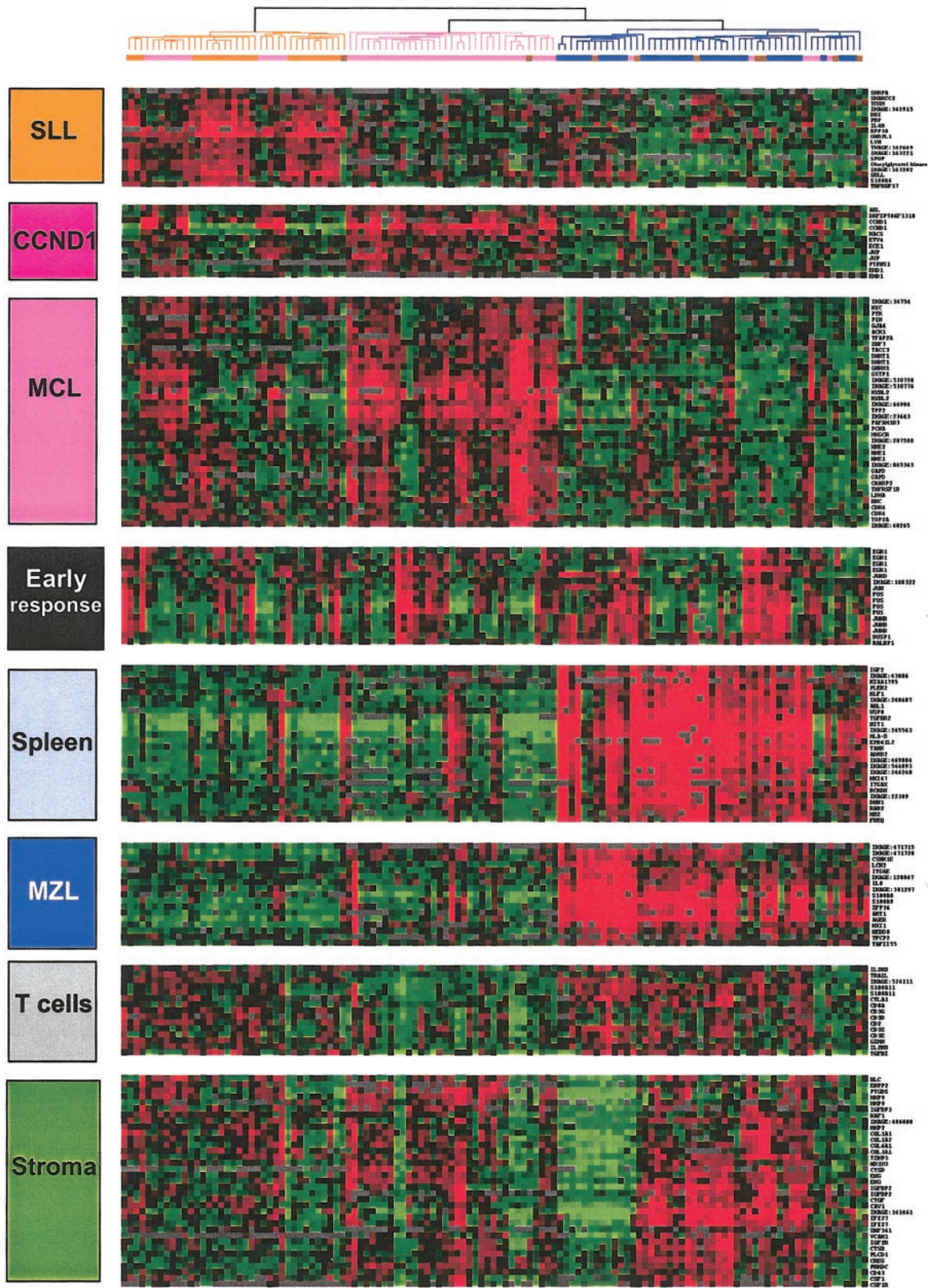


**Figure 2. Characteristic gene clusters.** Some of the correlated genes grouped into clusters and noted at the left side of the hierarchical clustering figures are reported. They correspond either to a specific type of contaminating cell (T cells) or a tissue type (stroma, spleen). The gene expression of 3 clusters were more specifically related to the 3 lymphoma entities: SLL, MZL, and MCL. SLL indicates small lymphocytic lymphoma; MZL, marginal zone lymphoma; MCL, mantle cell lymphoma; BC, borderline cases; CCND1, cyclin D1. Gene names are available on the *Blood* website as supplemental data (Table S1); see the Data Set link at the top of the online article.

correlation between individual samples and subtype mean profiles. It allowed a balanced selection of genes discriminating between lymphoma subtypes, and provided a sample prediction in more than 2 classes. Using this strategy, a minimal set of

44 genes from the SLL (16 genes), MCL (15 genes), MZL (9 genes), and CCND1 (4 genes) clusters were selected (Figure 3B). This set of genes included most of the best discriminating genes for the 3 lymphoma subtypes, and selection of larger

**Table 3. Distribution of the subtype-discriminating genes within specific clusters**

Gene-expression variable	No. of microarray features in signature n = 2532	No. of microarray features significantly associated ( $P < .00001$ ) with diagnosis of SLL n = 178	No. of microarray features significantly associated ( $P < .00001$ ) with diagnosis of MZL n = 83	No. of microarray features significantly associated ( $P < .00001$ ) with diagnosis of MCL n = 154	Representative genes	GenBank accession no.
SLL cluster	735	163	1	12	L-selectin	AJ246000
					IL4-R	C75499
					TNF-R17	
Cyclin D1 cluster	13	0	0	13	CCND1	NM_053056
MCL cluster	349	1	1	75	PCNA	AF508260
					CDK4	NM_007671
					MYBL2	
Early response cluster	20	0	0	0	Fos	V01512
Spleen cluster	54	0	36	0	HBZ	J00182
					KLF1	NM_006563
					EPB41L2	M_001431
MZL cluster	17	0	11	0	AKT1	AF283829
					AGER	NM_173982
					MX1	BC012907
T-cells cluster	15	0	4	0	CD3A	—
					CD3G	X06026
Stroma cluster	38	0	3	5	SPARC	J03040
					MMP9	J05079
Others	1291	14	27	49		—

— indicates no unique accession number.

sets of genes—up to 115 genes—gave very similar results (data not shown).

### Sample classification using the gene-expression-based diagnostic predictor

Correlations of individual samples with MCL and SLL mean profiles are shown in Figure 3A. The 19 SLL samples and the 27 splenic MZL samples formed homogeneous groups which were well separated from each other. Most of the MCL samples grouped together, but 3 of them shared MZL profiles and 2 samples could not be classified (see the 2 pink squares in the middle of the figure). All the borderline cases could be easily partitioned.

The validation group was blind analyzed. All the 10 SLL cases, 5 of the 8 MZL cases, and 8 of the 11 MCL cases were correctly classified in their respective entity. Two MCL samples exhibited an MZL gene-expression profile that ranked them with a predominant MZL score. Survival of these 5 misclassified MCL cases (3 in the preliminary group and 2 in the validation group) was not significantly different from that of the other patients with MCL although the median survival was more than 4.4 years (range, 2.3-5.6 years) compared with 2.6 years (range, 0.17-11.0 years) in the other MCL cases. Three MZL samples and one MCL sample in the validation group exhibited a profile that did not allow classification (Figure 3B). In these cases, hybridization signals were low, with gene-expression values that were not discriminant enough to determine a class prediction score.

The 6 borderline cases were analyzed separately. The 4 patients with borderline SLL-MZL clustered clearly within the MZL group and not in the SLL group. Among the 2 patients with borderline MCL-MZL, one clustered within the MCL group and the other within the MZL group. These data further demonstrated the interest for our genomic diagnostic-predictor for classifying borderline cases.

Patients with typical morphology but with presence of atypical cytogenetic or immunologic characteristics all fell into the appropriate category. Samples of the 2 patients with MZL with t(11;14) translocation, unmutated IgV<sub>H</sub> status, and cyclin D1 overexpression expressed the MZL hallmark genes such as AKT1, AGER, S100A proteins, and CCDN1 cluster genes but not the MCL hallmark genes such as proliferation genes or drug resistance genes signatures. In the 2-dimensional representation, these 2 patients were located inside the MZL group. The 5 splenic MZL cases expressing the CD5 marker and the 3 MCL cases lacking the CD5 marker expressed the expected signatures corresponding to their subtype and were in their correct group. The 2 nodal MZL cases were located inside the MZL group with high expression of the MZL gene signature, independently from the type of tissue biopsy. The 8 MCL cases with mutated IgV<sub>H</sub> presented a typical MCL profile. All MZL, SLL, and MCL samples presenting either mutated or unmutated IgV<sub>H</sub> status were grouped according to their histologic subtype.

### Immunohistochemistry results

We confirmed at the protein level that L-selectin was closely associated to SLL, AKT1 to MZL, and GST pi to MCL (Figure 4). L-selectin immunostaining showed a strong signal in all 5 SLL cases whereas no expression was detected in MZL and MCL cases. The 4 MZL/SLL borderline cases were all negative for L-selectin. GST pi immunostaining displayed a very strong signal in MCL samples whereas no expression was detected in MZL and detection in SLL was very weak as expected. Among the 2 MZL cases with t(11;14) one exhibited no GST pi expression whereas the other displayed very weak expression. The immunohistochemistry results of the 6 borderline cases were consistent with their genomic profile (data not shown). AKT1 immunostaining displayed a strong signal in MZL samples.







level of expression of genes whose function is related to induce resistance to apoptosis: *bcl-2*, already known as the major CLL dysregulation,<sup>21</sup> but also overexpression of other molecules such as survivin and TNFR10 known to have an antiapoptotic function. *Bax* expression was deregulated, which is consistent with what has been reported, *bax* expression being related to *bcl2* expression for the regulation of B-CLL cell survival.<sup>22</sup> In addition to genes preventing cell death, an overexpression of several genes encoding cell cycle proteins such as cyclin D2, D3, and cyclin H was found in these low-rate proliferating cells. The IL4 receptor pathway was overexpressed in all SLL samples as has been reported in CLL analysis.<sup>8</sup> IL4 receptor is the ligand for IL4 that promotes B-cell growth and survival via transcription nuclear factor (NF)- $\kappa$ B.<sup>23</sup> IL4 receptor stimulation is also known to induce CD23 expression<sup>24</sup> which is a marker of the SLL/CLL cells.

Comparison of gene-expression profiles between B-CLL reported in several studies<sup>6,8,25</sup> and SLL in our study showed that patients with B-CLL and patients with SLL shared a common gene signature, including L-selectin and P-selectin, titin, IL4 receptor, CCR, adenylate kinase, diacylglycerol kinase, cyclin D2, and *bcl-2* overexpression. This suggests a common normal cell precursor, suggested by others to be related to memory B cells.<sup>6,8</sup>

Splenic marginal zone B-cell lymphomas were specifically characterized by the overexpression of a gene cluster containing AKT1, which is localized in a hot spot region for chromosomal abnormalities in lymphomas: 14q32.3. AKT1 is a serine threonine kinase and belongs to a major cell survival pathway, the PI 3-kinase/AKT pathway that regulates survival of many cells by inhibiting the action of certain proapoptotic proteins (BAD, FKHR, caspase 9).<sup>26</sup> In the same gene cluster, the analysis showed S100A proteins and AGER grouped together with the same overexpression among the MZL samples. S100 proteins belong to a group of EF-hand calcium-binding proteins and are polypeptides present at sites of inflammation. Expression of S100A11 has been reported to be elevated in colorectal cancer compared with normal colorectal mucosa<sup>27</sup>, and in breast cancer-derived metastatic axillar lymph nodes compared with normal lymph nodes or breast fibroadenomas.<sup>28</sup> It has been demonstrated that AKT1 is involved in the regulation of S100A protein expression.<sup>29</sup> AGER (advanced glycosylation end product-specific receptor) protein, or RAGE, is a multiligand member of the immunoglobulin superfamily,<sup>30</sup> and particularly a central receptor for the S100/calgranulin superfamily.<sup>31</sup> Engagement of RAGE by a ligand activates key cell signaling pathways, such as p21<sup>(ras)</sup>, MAP kinases, NF- $\kappa$ B, and *cdc42/rac*.<sup>32,33</sup> Expression of several other genes related to transcription were significantly correlated in this AKT1 cluster, such as ZFP36 which codes for a zinc finger protein related with TNF $\alpha$  induced-inflammatory process, MXI1, a max-interacting protein, and TFCP2, a transcription factor for CP2 interacting with the alpha-globin gene promotor.<sup>34</sup>

Comparison of the MCL-specific signature to SLL and MZL signatures showed high levels of expression of cell cycle progression genes that function in the G1 phase, such as cyclin D1 and CDK4, as well as in the G2/M phase, such as cyclin F, or in both, such as PCNA, responsible for controlling the transition from G1 phase to the S phase and from the G2 phase to the M phase. This deregulation of several genes that are involved at different points of the cell cycle is in accordance with studies reporting that overexpressed cyclin D1 in MCL cooperates with

other regulatory cell cycle genes.<sup>7,35,36</sup> Moreover, when considering MCL analysis, clustering resulted in the separation of 2 signatures: the cyclin D1 signature and a signature including all the other MCL genes. This suggests that, if cyclin D1 overexpression is important and considered as characteristic of MCL, cyclin D1 overexpression is not sufficient alone to provide an MCL phenotype and that the control of cyclin D1 expression is independent from that of other MCL-specific genes. This result is in accordance with the existence of cyclin-D1-negative MCL recently reported.<sup>7</sup> In this case, entry into S phase is suggested to depend on the overexpression of other cyclins such as cyclin D2 or cyclin D3.<sup>7</sup> We observed in every case that gene-expression-increased cell cycle activity was correlated to an overexpression of genes encoding for protein machinery (actin beta and gamma genes; TUBB2, beta 2-tubulin gene; DDBN1 or Debrin1, an actin-binding protein involved in the regulation of the growth process; BMP4 or bone morphogenetic protein 4, SMARCA 4 an actin-dependent regulator of chromatin) and, in parallel, genes encoding for cell proliferation (FYN, ABL, PTK, and kit encoding for tyrosine kinase proteins). Interestingly, several genes encoding for membrane transporters and implicated in drug resistance were found to be overexpressed: 2 GST pi and 2 MDR/ATP-binding cassette (ABC) membrane proteins (ABCG2 and ABCC5). The gene GST pi is located on chromosome 11,<sup>37</sup> very close to *Bcl1*, and has been suggested<sup>38</sup> to be rearranged within the t(11;14) translocation characterizing MCLs.<sup>39</sup> This overexpression of several genes related to multidrug resistance is consistent with the known MCL clinical evolution which is marked by treatment failure leading to fatal recurrence with a median survival close to 3 years.<sup>40</sup>

#### Genomic profiling and clinical implications for SLL, splenic MZL, and MCL

Our study allowed us to distinguish with great precision the SLL, splenic MZL, and MCL entities with 44 genes grouped into 4 gene-expression signatures. We were able to classify each patient by using a score that allowed us to perform a genomic prediction of the diagnosis.

Several samples in our series were either borderline cases, which occur in routine practice,<sup>10,41</sup> or cases exhibiting atypical immunophenotypic or cytogenetic characteristics. The analysis of the 6 borderline cases displayed specific MZL or MCL genomic profiles without any ambiguity that were consistent with the clinical outcome of the patients. Histologic immunostaining using the 3 selected antibodies (GST pi, L-selectin analysis) showed consistent results with the respective genomic score obtained in these borderline cases.

The translocation t(11;14)(q13;q32) has been described in about 15% of patients with splenic MZL.<sup>42-44</sup> This feature is considered to be characteristic of MCL although it can also be seen in plasma-cell leukemia, multiple myeloma, hairy cell leukemias, and B-prolymphocytic leukemia,<sup>45</sup> and is missing in MCL.<sup>7,46</sup> We have demonstrated that the cyclin D1 signature was a feature independent from the MCL signature. Interestingly, and confirming these data, the 2 splenic MZL samples exhibiting a t(11,14)(q13;q32) translocation shared a common genomic profile with that of the typical MZL samples. None of the genes specific for the MCL signature except cyclin D1 were expressed in these 2 MZL samples. Furthermore, expression values of GST pi transcript whose gene is located near the cyclin D1 locus were not as elevated as GST pi expression values in the MCL samples (data not shown), as confirmed by the lack or weak expression of

GST pi protein in these samples. This supports the hypothesis of different bcl-1 breakpoints in MCL and in MZL.<sup>44,47</sup> The existence of a t(11;14) translocation in MZL does not seem to induce a more aggressive clinical course (Troussard et al<sup>44</sup> and C. T., personal data, February 2003) supporting the hypothesis that occurrence of t(11,14) in MZL should not suffice to alter diagnostic classification or to consider these t(11;14)-positive patients with MZL as a distinct lymphoma group.

The development of a specific microarray with 44 genes could be proposed as a supplementary tool in routine practice. Our results showed that 4 samples (3%) were not classified using the genomic predictor because of poor quality of RNA. In clinical practice, obtaining high-quality RNA for all samples is difficult. Investigations at the protein level could be an easier way. The use of supplementary markers, such as the 3 selected in our study—after confirmation of the presented preliminary results—in addition to the classical immunostaining panel for B-cell lymphomas diagnosis might be considered in pathology laboratories, in order to improve the diagnosis of B-cell lymphomas.

## References

- Alizadeh A, Eisen M, Davis R, et al. Distinct types of diffuse large B-cell lymphoma identified by gene expression profiling. *Nature*. 2000;403:491-492.
- Rosenwald A, Wright G, Chan W, et al. The use of molecular profiling to predict survival after chemotherapy for diffuse large-B-cell lymphoma. *N Engl J Med*. 2002;346:1937-1947.
- Shipp M, Ross K, Tamayo P, et al. Diffuse large B-cell lymphoma outcome prediction by gene expression profiling and supervised machine learning. *Nat Med*. 2002;8:68-74.
- Shaffer A, Rosenwald A, Staudt L. Lymphoid malignancies: the dark side of B-cell differentiation. *Nat Rev Immunol*. 2002;2:920-932.
- Berger F, Felman P, Sonet A, et al. Nonfollicular small B-cell lymphomas: a heterogeneous group of patients with distinct clinical features and outcome. *Blood*. 1994;83:2829-2835.
- Rosenwald A, Alizadeh A, Widhopf G, et al. Relation of gene expression phenotype to immunoglobulin mutation genotype in B cell chronic lymphocytic leukemia. *J Exp Med*. 2001;194:1639-1647.
- Rosenwald A, Wright G, Wiestner A, et al. The proliferation gene expression signature is a quantitative integrator of oncogenic events that predicts survival in mantle cell lymphoma. *Cancer Cell*. 2003;3:185-197.
- Klein U, Tu Y, Stolovitzky G, et al. Gene expression profiling of B cell chronic lymphocytic leukemia reveals a homogeneous phenotype related to memory B cells. *J Exp Med*. 2001;194:1625-1638.
- Jaffe E, Harris N, Stein H, Vardiman J. World Health Organization Classification of Tumours: Tumours of Haematopoietic and Lymphoid Tissues. Lyon, France: IARC; 2001.
- Thieblemont C, Felman P, Callet-Bauchu E, et al. Splenic marginal-zone lymphoma: a distinct clinical and pathological entity. *Lancet Oncol*. 2003;4:95-103.
- Uchimaru K, Taniguchi T, Yoshikawa M, et al. Detection of cyclin D1 (bcl-1, PRAD1) overexpression by a simple competitive reverse transcription-polymerase chain reaction assay in t(11;14)(q13;q32)-bearing B-cell malignancies and/or mantle cell lymphoma. *Blood*. 1997;89:965-974.
- Traverse-Glehen A, Berger F, Davi F, et al. Analysis of VH genes in 48 marginal zone lymphoma cases reveals marked heterogeneity between splenic and nodal cases and suggest clonal selection [abstract]. *Blood*; 2002;100:568a.
- Bertucci F, Houlgatte R, Benziane A, et al. Gene expression profiling of primary breast carcinomas using arrays of candidate genes. *Hum Mol Genet*. 2000;9:2981-2991.
- Bertucci F, Bernard K, Loric B, et al. Sensitivity issues in DNA array-based expression measurements and performance of nylon microarrays for small samples. *Hum Mol Genet*. 1999;8:219-226.
- Eisen M, Spellman P, Brown P, Botstein D. Cluster analysis and display of genome-wide expression patterns. *Proc Natl Acad Sci U S A*. 1998;95:14863-14868.
- Golub T, Slonim D, Tamayo P, et al. Molecular classification of cancer: class discovery and class prediction by gene expression monitoring. *Science*. 1999;286:531-537.
- Magrangeas F, Nasser V, Avet-Loiseau H, et al. Gene expression profiling of multiple myeloma reveals molecular portraits in relation to the pathogenesis of the disease. *Blood*. 2003;101:4998-5006.
- Bland J, Altman D. Multiple significance tests: the Bonferroni method. *BMJ*. 1995;310:170.
- Sorlie T, Perou C, Tibshirani R, et al. Gene expression patterns of breast carcinomas distinguish tumor subclasses with clinical implications. *Proc Natl Acad Sci U S A*. 2001;98:10869-10874.
- Takahashi M, Rhodes D, Furge K, et al. Gene expression profiling of clear cell renal cell carcinoma: gene identification and prognostic classification. *Proc Natl Acad Sci U S A*. 2001;98:9754-9759.
- Schena M, Larsson L, Gottardi D, et al. Growth and differentiation-associated expression of bcl-2 in B-chronic lymphocytic leukemia cells. *Blood*. 1992;79:2981-2989.
- Aguilar-Santelises M, Rottenberg M, Lewin N, Mellstedt H, Jondal M. Bcl-2, Bax and p53 expression in B-CLL in relation to in vitro survival and clinical progression. *Int J Cancer*. 1996;69:114-119.
- Zaninoni A, Imperiali F, Pasquini C, Zanella A, Barcellini W. Cytokine modulation of nuclear factor-kappaB activity in B-chronic lymphocytic leukemia. *Exp Hematol*. 2003;31:185-190.
- Punnonen J, Aversa G, Cocks B, de Vries J. Role of interleukin-4 and interleukin-13 in synthesis of IgE and expression of CD23 by human B cells. *Allergy*. 1994;49:576-586.
- Thieblemont C, Chettab K, Felman P, et al. Identification and validation of seven genes, as potential markers, for the differential diagnosis of small B cell lymphomas (small lymphocytic lymphoma, marginal zone B cell lymphoma and mantle cell lymphoma) by cDNA macroarrays analysis. *Leukemia*. 2002;16:2326-2329.
- Vivanco I, Sawyers C. The phosphatidylinositol 3-kinase AKT pathway in human cancer. *Nat Rev Cancer*. 2002;7:489-501.
- Tanaka M, Adzuma K, Iwami M, Yoshimoto K, Monden Y, Itakura M. Human calgizzarin: one colorectal cancer-related gene selected by a large scale random cDNA sequencing and northern blot analysis. *Cancer Lett*. 1995;89:195-200.
- Tomasetto C, Regnier C, Moog-Lutz C, et al. Identification of four novel human genes amplified and overexpressed in breast carcinoma and localized to the q11-q21.3 region of chromosome 17. *Genomics*. 1995;28:367-376.
- Hernan R, Fasheh R, Calabrese C, et al. ERBB2 up-regulates S100A4 and several other prometastatic genes in medulloblastoma. *Cancer Res*. 2003;63:140-148.
- Neeper M, Schmidt A, Brett J, et al. Cloning and expression of a cell surface receptor for advanced glycosylation end products of proteins. *J Biol Chem*. 1992;267:14998-15004.
- Hofmann M, Drury S, Fu C, et al. RAGE mediates a novel proinflammatory axis: a central cell surface receptor for S100/calgranulin polypeptides. *Cell*. 1999;97:889-901.
- Lander H, Tauras J, Ogiste J, Hori O, Moss R, Schmidt A. Activation of the receptor for advanced glycation end products triggers a p21(ras)-dependent mitogen-activated protein kinase pathway regulated by oxidant stress. *J Biol Chem*. 1997;272:17810-17814.
- Huttunen H, Fages C, Rauvala H. Receptor for advanced glycation end products (RAGE)-mediated neurite outgrowth and activation of NF-kappaB require the cytoplasmic domain of the receptor but different downstream signaling pathways. *J Biol Chem*. 1999;274:19919-19924.
- Swendeman S, Spielholz C, Jenkins N, Gilbert D, Copeland N, Sheffery M. Characterization of the genomic structure, chromosomal location, promoter, and development expression of the alpha-globin transcription factor CP2. *J Biol Chem*. 1994;269:11663-11671.
- Hofmann W, de Vos S, Tsukasaki K, et al. Altered apoptosis pathways in mantle cell lymphoma detected by oligonucleotide microarray. *Blood*. 2001;98:787-794.
- de Vos S, Krug U, Hofmann W, et al. Cell cycle alterations in the blastoid variant of mantle cell



- lymphoma (MCL-BV) as detected by gene expression profiling of mantle cell lymphoma (MCL) and MCL-BV. *Diagn Mol Pathol*. 2003;12:35-43.
37. Laisney V, Nguyen Van C, Gross M, Frezal J. Human genes for glutathione S-transferases. *Hum Genet*. 1984;68:221-227.
  38. Ribrag V, Fadel I, Cebotaru C, et al. High level of glutathione-S-transferase pi expression in mantle cell lymphomas [abstract]. *Blood*. 1999;94:65a.
  39. Barista I, Romaguera J, Cabanillas F. Mantle-cell lymphoma. *Lancet Oncol*. 2001;2:141-148.
  40. Samaha H, Dumontet C, Ketterer N, et al. Mantle cell lymphoma: a retrospective study of 121 cases. *Leukemia*. 1998;12:1281-1287.
  41. Gupta D, Lim M, Medeiros L, Elenitoba-Johnson K. Small lymphocytic lymphoma with perifollicular, marginal zone, or interfollicular distribution. *Mod Pathol*. 2000;13:1161-1166.
  42. Oscier DG, Matutes E, Gardiner A, et al. Cytogenetic studies in splenic lymphoma with villous lymphocytes. *Br J Haematol*. 1993;85:487-491.
  43. Jadayel D, Matutes E, Dyer M, et al. Splenic lymphoma with villous lymphocytes: analysis of bcl-1 rearrangements and expression of the cyclin D1 gene. *Blood*. 1994;83:3664-3671.
  44. Troussard X, Mauvieux L, Radford-Weiss I, et al. Genetic analysis of splenic lymphoma with villous lymphocytes: a Groupe Francais d'Hematologie Cellulaire (GFHC) study. *Br J Haematol*. 1998;101:712-721.
  45. Brito-Babapulle V, Ellis J, Matutes E, et al. Translocation t(11-14)(q13-q32) in chronic lymphoid disorders. *Genes Chromosomes Cancer*. 1992;5:158-165.
  46. Yatabe Y, Suzuki R, Tobinai K, et al. Significance of cyclin D1 overexpression for the diagnosis of mantle cell lymphoma: a clinicopathologic comparison of cyclin D1-positive MCL and cyclin D1-negative MCL-like B-cell lymphoma. *Blood*. 2000;95:2253-2261.
  47. Cuneo A, Bardi A, Wlodarska I, et al. A novel recurrent translocation t(11;14)(p11;q32) in splenic marginal zone B cell lymphoma. *Leukemia*. 2001;15:1262-1267.
  48. Wu E, Aguiar R, Savage K, et al. PKC $\beta$ : a rational therapeutic target in diffuse large B-cell lymphoma [abstract]. *Blood*. 2002;100:202a.